Higher-order defect-mode laser in an optically thick photonic crystal slab

Se-Heon Kim,[1,3,*] Jingqing Huang,[2,3] and Axel Scherer[1,2,3]

[1]*Department of Physics, California Institute of Technology, Pasadena, California 91125, USA*

[2]*Department of Electrical Engineering, California Institute of Technology, Pasadena, California 91125, USA*

[3]*Kavli Nanoscience Institute, California Institute of Technology, Pasadena, California 91125, USA*

**Corresponding author: seheon@caltech.edu*

Received October 26, 2012; revised November 29, 2012; accepted December 3, 2012;
posted December 6, 2012 (Doc. ID 178784); published January 7, 2013

The use of an optically thick slab may provide versatile solutions for the realization of a current injection-type laser using photonic crystals. Here, we show that a transversely higher-order defect mode can be designed to be confined by a photonic bandgap in such a thick slab. Using simulations, we show that a high Q of $>10^5$ is possible from a finely tuned second-order hexapole mode (2h). Experimentally, we achieve optically pumped pulsed lasing at 1347 nm from the 2h with a peak threshold pump power of 88 μW.

OCIS codes: 230.5298, 250.5960.

Two-dimensional (2-D) photonic crystal (PhC) slab structures have, so far, been in the form of a thin dielectric slab whose thickness T is often chosen to be ~200 nm for an operational wavelength of ~1.3 μm. This thickness consideration is to maximize the size of the photonic bandgap (PBG) in the in-plane direction (x–y plane) [1], which has unfortunately placed a severe constraint on the design of a current-injection type laser. Pulsed lasing operation has been demonstrated using a vertically varying p-i-n doping structure within the thin PhC slab, for which a submicrometer-size dielectric post placed directly underneath the laser cavity serves as a current path [2]. Recent efforts have moved toward a *laterally* varying p-i-n structure, and a few successful results were already reported by groups in both Stanford [3] and Nippon Telegraph and Telephone Corporation (NTT) [4]. However, there are still favorable reasons for using a vertically varying doped structure because such a design allows a monolithic growth of all of the epitaxial layers that are almost free of crystal defects.

Recently, we have shown that even a very thick slab can support sufficiently high-Q (few thousands) cavity modes for lasing [5]. In our previous result, however, the dipole mode formed in a triangular-lattice air-hole PhC slab was emitting more photons into the in-plane directions than into the vertical direction (z) for efficient photon emission and collection. Moreover, Q could not exceed 3000 with $T = 606$ nm. It would seem, at first, that we have no other options for further improvement in Q because the poor horizontal confinement appears inevitable due to the absence of a PBG. It is our purpose in this Letter to rebut this first intuition and show that the thick slab can be used to achieve an efficient vertical emitter with a surprisingly high Q of over 10^5.

To start, we perform numerical simulations using both the plane-wave-expansion method [6] and the finite-difference time-domain (FDTD) method to investigate how a PBG evolves as we change the air-hole radius (r) and the slab thickness (T) [Fig. 1(a)]. Note that r and T are represented in the unit of the lattice constant (a). In the case of a triangular-lattice air-hole PhC, $\{r = 0.40a, T = 0.6a\}$ gives the widest gap centered at $\omega_c \approx 0.38$, which agrees with earlier work by Johnson *et al.* [1]. Also note that there exists a broad region of $\{r, T\}$ that gives a wide gap-to-midgap ratio [1] $\widetilde{\Delta\omega} > 30\%$. This is why r and T are often chosen to be ~$0.35a$ and $0.5a$, respectively. We also find that a tiny PBG (usually $\widetilde{\Delta\omega} \sim 1\%$) exists up to $T = 1.25a$.

The dipole mode discussed in our previous work [5] ($T = 1.86a$) is marked as "1d" in the gap map. Now, we pose the question of whether we can design a certain resonant mode emitting at ~1.3 μm that is confined by a PBG in a slab with $T = 606$ nm. From the gap map diagram, the only possibility appears to be increasing a in order to bring down $T(a)$ below $1.25a$. However, keeping the same 1d mode, larger a usually results in longer λ because $\omega = a/\lambda$ is rather fixed by the in-plane modal structure of a resonant mode [7]. Therefore, we should look instead into other resonant modes that do not resemble the dipole mode.

It is well known that even a single-defect resonator supports multiple resonances such as the quadrupole, the hexapole, and the monopole modes [8]. These higher-order modes are pulled down from the conduction-band edge of the photonic band structure [7]. Further tuning the defect region can get more higher-order modes pulled down into the gap. One possible route from the (first-order) dipole mode (1d) to the second-order hexapole mode ("2h") is drawn by an arrow in the gap map diagram. The 2h mode is designed to be resonant at a wavelength close to that of 1d (Structural parameters for this second hexapole mode are as follows: $K_1 = 1.07a$, $K_2 = 0.99a$, $R_1 = 0.28a$, $R_{bg} = 0.46a$, $R = 0.46a$. For definitions of these parameters, see Fig. 2.) even though it has quite a large a of 500 nm (thus, $T \approx 1.21a$). As a quantitative measure showing how well the PhC layers work as a mirror, we calculate the vertical extraction efficiency η_{vert} defined by $\eta_{vert} \equiv (1/Q_{vert})/(1/Q_{horz} + 1/Q_{vert}) = (1/Q_{vert})/(1/Q_{tot})$ [5]. We find that η_{vert} of 2h shown in Fig. 1(c) is 0.954 ($Q_{horz} = 3.3 \times 10^5$) with the same number of air-hole barriers shown in Fig. 2(b). We believe this η_{vert} (or Q_{horz}) has not yet been saturated due to the small gap size, expecting further improvement by increasing the number of barriers. Probably, in applying the idea of a higher-order resonant mode, T of 606 nm would be

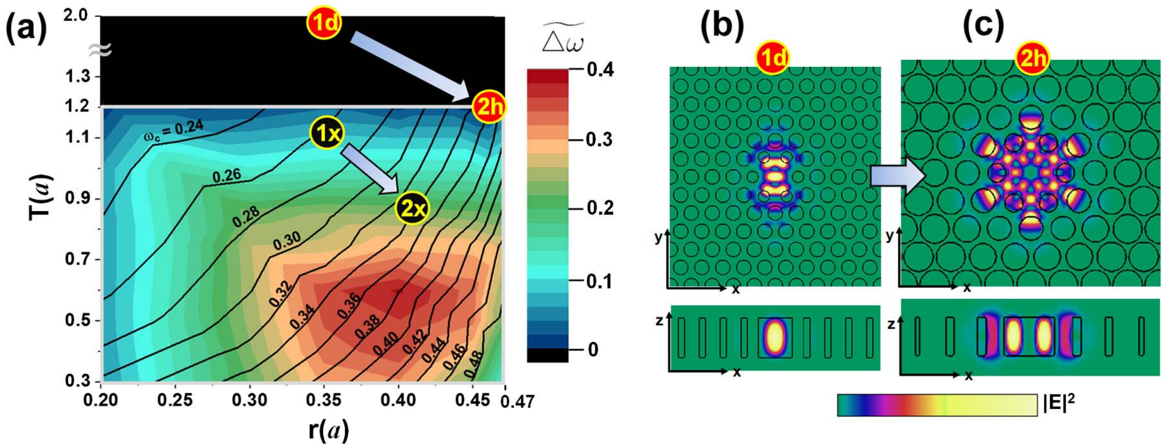

Fig. 1. (Color online) (a) 2-D map of a PBG for a triagular-lattice air-hole (radius = r) PhC in a dielectric slab ($n_{\mathrm{slab}} = 3.4$) with a thickness of T. The 2-D color scale map represents the size of the PBG in terms of the gap-to-midgap ratio defined by $\widetilde{\Delta\omega} \equiv \Delta\omega/\omega_c$, where ω_c is the center frequency of a PBG. The contour curves of ω_c are overlaid on the 2-D map. Note that throughout the Letter, all frequencies are normalized by $2\pi c/a$; hence $\omega = a/\lambda$ (dimensionless). (b) First-order dipole mode (1d) [$Q = 2600$ and $V = 0.82(\lambda/n_{\mathrm{slab}})^3$] oscillating at $\lambda = 1341$ nm with $a = 325$ nm. (c) Second-order hexapole mode (2h) [$Q = 15{,}200$ and $V = 2.23(\lambda/n_{\mathrm{slab}})^3$] oscillating at $\lambda = 1365$ nm with $a = 500$ nm. Both modes are formed in a slab with $T = 606$ nm.

the upper limit for $\lambda \sim 1300$ nm, as 2h can only be made barely located at the top-right corner of the gap map diagram. We would like to note that the same strategy can be applied more effectively to the case of an intermediate thickness range of 400 nm $< T <$ 600 nm. Imagine a first-order resonant mode ("1x") oscillating at $\omega \approx 0.26$ within a slab with $T = 1.1a$. At this region, $\widetilde{\Delta\omega}$ is only about 5%. We can bring it down deep into the bandgap by utilizing its second-order resonant mode ("2x"). If 2x oscillates at $\omega \approx 0.33$, then, without altering λ, 2x can be formed in a slab with $T \approx 0.87a$, at which $\widetilde{\Delta\omega}$ is as large as 20%.

Note that when choosing structural parameters for 2h we intend to obtain higher ω rather than higher Q. This is to minimize $T(a)$ so as to create a PBG. However, 2h requires the large air holes of $R = 0.46a$ to locate its resonance at the center of the tiny bandgap, which is not advantageous for the device's mechanical robustness. Therefore, we proceed to study if the background air-hole radii (R_{bg}) can be substantially reduced without sacrificing Q too much. $R_1 = 0.26a$, $K_1 = 1.07a$, and $K_2 = 1.04a$ [See Fig. 2(a)] have been chosen to optimize Q. As a result, ω decreases by about 10% in comparison with the case shown in Fig. 1(c). Several representative cases of fine-tuned air holes are shown in Fig. 2 and Table 1. The outskirt region from R_4 is intended as a mirror. Air-hole radii before and after R_4 are designed to vary gradually to minimize unintentional scattering losses at the crystal dislocations. Because R_1, K_1, and K_2 are fixed, all the resonant wavelengths tend to stay near 1323 nm. $a = 450$ nm for all those cases, thus $T = 1.35a$ and there exists no PBG.

Contrary to the initial expectation, Q can be made higher even in the absence of a rigorous PBG. In Case II, we find that Q_{vert} can be greatly improved by more than a factor of 10, and thereby Q_{tot} can reach over 10^5. It is interesting to observe that, comparing cases I and II, air holes located far from the mode's energy ($R_{>6}$) can affect Q_{vert}. It should also be noted that just one layer of $R_4 = 0.45a$ effectively blocks the horizontal photon leakage. As we progressively reduce R, both Q_{vert} and Q_{horz} decrease somewhat. However, all cases show quite high $\eta_{\mathrm{vert}} > \sim 0.8$ even in the absence of a PBG, which seems to imply that a careful engineering of the background air holes (such as hole-size chirping) can reduce the coupling loss between the defect mode and the in-plane Bloch modes [9].

In experiment, we intend to fabricate a structurally more robust design similar to case VI rather than the

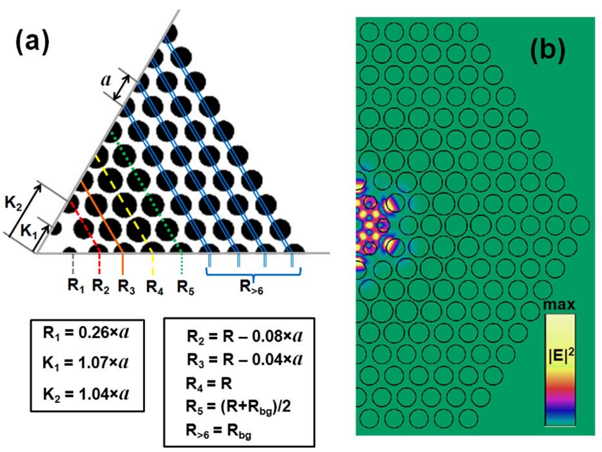

Fig. 2. (Color online) (a) Schematic diagram shows how we finely tune air-hole sizes and locations to optimize Q. (b) Electric-field intensity distribution ($|E|^2$) of the highest-Q mode (case II in Table 1).

Table 1. Examples of the Second-Order Hexapole Mode in a $T = 606$ nm Slab

Case	$R(a)$	$R_{\mathrm{bg}}(a)$	Q_{tot}	Q_{vert}	η_{vert}
I	0.45	0.45	55,400	58,500	0.947
II	0.45	0.38	105,100	146,200	0.719
III	0.44	0.38	50,400	63,900	0.789
IV	0.43	0.38	27,900	34,400	0.811
V	0.42	0.38	17,800	21,800	0.813
VI	0.41	0.38	12,400	15,300	0.807

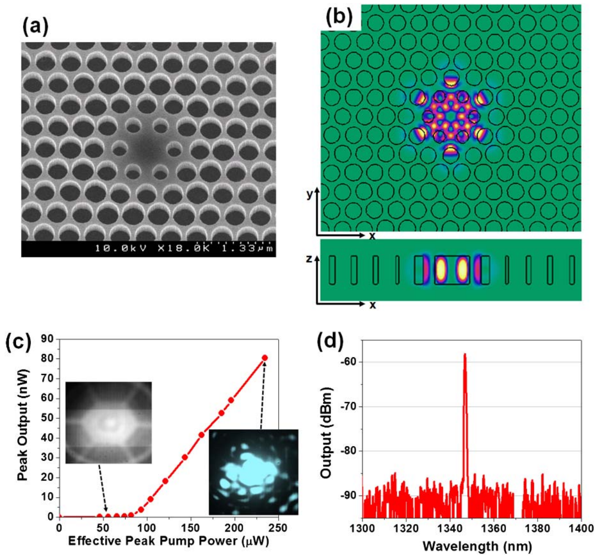

Fig. 3. (Color online) (a) SEM image taken at a tilt of about 10°. Note that $T = 606$ nm. (b) FDTD simulated mode profile. (c) Light-in versus light-out (*L–L*) curve. Insets show near-infrared camera images taken before and after the lasing. (d) Lasing spectrum measured at a peak pump power of 200 μW.

Q-optimized design of case II. We use the same InGaAsP wafer containing seven InGaAsP quantum wells emitting near 1325 nm used in our previous work [5]. To define high-aspect-ratio air holes, we use chemically assisted ion-beam etching with Ar and Cl_2 [5]. The fabricated devices are optically pumped at room temperature with a 830 nm laser diode driven by a pulse generator at 1 MHz with a duty cycle of 2.5%. A 100× objective lens is used to focus the pump laser on the center of the resonator (pump spot size ~3.5 μm). The *L–L* curve in Fig. 3(c) clearly shows a threshold, estimated to be 88 μW in terms of peak pump power, where we have assumed about 20% of actual incident pump power is absorbed by the slab. In Fig. 3(d), we verify single-mode lasing operation over a wide spectral range (1300–1400 nm) with a side-mode suppression ratio of ~30 dB. To confirm if the measured laser peak truly originates from the 2h mode, we perform FDTD simulation using a contour input for actual fabricated air holes from the scanning-electron microscopy (SEM) image [see Fig. 3(b)]. The FDTD expects that the designed 2h mode should locate at a wavelength of 1340 nm, which agrees very well with the experimental result. However, the FDTD expects somewhat lower Q of ~3000, which could be due to the slightly broken six-fold symmetry in the six nearest neighboring holes (R_1).

Finally, one feasible design for the realization of a current-injection laser is to insert a thin sacrificial layer in the middle of the thick slab, which is to be wet-chemically removed to form a current aperture. The thick slab enables a mechanically robust double slab in the form of a vertically varying *p-i-n* structure [10].

This work was supported by DARPA under NACHOS (W911NF-07-1-0277) and by the National Science Foundation under NSF CIAN ERC (EEC-0812072).

References

1. S. G. Johnson, S. Fan, P. R. Villeneuve, J. D. Joannopoulos, and L. A. Kolodziejski, Phys. Rev. B **60**, 5751 (1999).
2. H.-G. Park, S.-H. Kim, S.-H. Kwon, Y.-G. Ju, J.-K. Yang, J.-H. Baek, S.-B. Kim, and Y.-H. Lee, Science **305**, 1444 (2004).
3. B. Ellis, M. A. Mayer, G. Shambat, T. Sarmiento, J. Harris, E. E. Haller, and J. Vuckovic, Nat. Photonics **5**, 297 (2011).
4. S. Matsuo, K. Takeda, T. Sato, M. Notomi, A. Shinya, K. Nozaki, H. Taniyama, K. Hasebe, and T. Kakitsuka, Opt. Express **20**, 3773 (2012).
5. S.-H. Kim, J. Huang, and A. Scherer, Opt. Lett. **37**, 488 (2012).
6. S. Johnson and J. Joannopoulos, Opt. Express **8**, 173 (2001).
7. J. D. Joannopoulos, S. G. Johnson, J. N. Winn, and R. D. Meade, *Photonic Crystals: Molding the Flow of Light*, 2nd ed. (Princeton University, 2008).
8. H.-G. Park, J.-K. Hwang, J. Huh, H.-Y. Ryu, S.-H. Kim, J.-S. Kim, and Y.-H. Lee, IEEE J. Quantum Electron. **38**, 1353 (2002).
9. S.-H. Kim, A. Homyk, S. Walavalkar, and A. Scherer, "High-Q impurity photon states bounded by a photonic-band-pseudogap in an optically-thick photonic-crystal slab," http://arxiv.org/abs/1209.5726.
10. S. Kim, A. Scherer, J. Huang, and D. Y. Oh, "Chemical-etched nanostructures and related devices," U.S. patent application US2012/0153260A1 (June 21, 2012).